



TECH BRIEFS

NATIONAL AERONAUTICS AND SPACE ADMINISTRATION

-  Technology Focus
-  Electronics/Computers
-  Software
-  Materials
-  Mechanics/Machinery
-  Manufacturing
-  Bio-Medical
-  Physical Sciences
-  Information Sciences
-  Books and Reports
-  Green Design

INTRODUCTION

Tech Briefs are short announcements of innovations originating from research and development activities of the National Aeronautics and Space Administration. They emphasize information considered likely to be transferable across industrial, regional, or disciplinary lines and are issued to encourage commercial application.

Availability of NASA Tech Briefs and TSPs

Requests for individual Tech Briefs or for Technical Support Packages (TSPs) announced herein should be addressed to

National Technology Transfer Center

Telephone No. **(800) 678-6882** or via World Wide Web at **www.nttc.edu**

Please reference the control numbers appearing at the end of each Tech Brief. Information on NASA's Innovative Partnerships Program (IPP), its documents, and services is also available at the same facility or on the World Wide Web at **<http://www.nasa.gov/offices/ipp/network/index.html>**

Innovative Partnerships Offices are located at NASA field centers to provide technology-transfer access to industrial users. Inquiries can be made by contacting NASA field centers listed below.

Ames Research Center
Mary Walsh
(650) 604-1405
mary.w.walsh@nasa.gov

Dryden Flight Research Center
Yvonne D. Gibbs
(661) 276-3720
yvonne.d.gibbs@nasa.gov

Glenn Research Center
Joe Shaw, Acting Chief
(216) 977-7135
robert.j.shaw@nasa.gov

Goddard Space Flight Center
Nona Cheeks
(301) 286-5810
nona.k.cheeks@nasa.gov

Jet Propulsion Laboratory
Indrani Graczyk
(818) 354-2241
indrani.graczyk@jpl.nasa.gov

Johnson Space Center
information
(281) 483-3809
jsc.techtran@mail.nasa.gov

Kennedy Space Center
David R. Makufka
(321) 867-6227
david.r.makufka@nasa.gov

Langley Research Center
Elizabeth B. Plentovich
(757) 864-2857
elizabeth.b.plentovich@nasa.gov

Marshall Space Flight Center
Jim Dowdy
(256) 544-7604
jim.dowdy@msfc.nasa.gov

Stennis Space Center
Ramona Travis
(228) 688-3832
ramona.e.travis@nasa.gov

Carl Ray, Program Executive
Small Business Innovation
Research (SBIR) & Small
Business Technology
Transfer (STTR) Programs
(202) 358-4652
carl.g.ray@nasa.gov

Doug Comstock, Partnerships
Innovation and Commercial
Space Program Office (formerly IPP)
(202) 358-2221
doug.comstock@nasa.gov



TECH BRIEFS

NATIONAL AERONAUTICS AND SPACE ADMINISTRATION



5 Technology Focus: Data Acquisition

- 5 Wind and Temperature Spectrometry of the Upper Atmosphere in Low-Earth Orbit
- 5 Health Monitor for Multitasking, Safety-Critical, Real-Time Software
- 6 Stereo Imaging Miniature Endoscope
- 7 Early Oscillation Detection Technique for Hybrid DC/DC Converters
- 7 Parallel Wavefront Analysis for a 4D Interferometer



9 Electronics/Computers

- 9 Schottky Heterodyne Receivers With Full Waveguide Bandwidth
- 9 Carbon Nanofiber-Based, High-Frequency, High-Q, Miniaturized Mechanical Resonators
- 10 Ultracapacitor-Based Uninterrupted Power Supply System
- 11 Coaxial Cables for Martian Extreme Temperature Environments
- 11 Using Spare Logic Resources To Create Dynamic Test Points



13 Software

- 13 Autonomous Coordination of Science Observations Using Multiple Spacecraft
- 13 Autonomous Phase Retrieval Calibration
- 13 EOS MLS Level 1B Data Processing Software, Version 3
- 14 Cassini Tour Atlas Automated Generation
- 14 Software Development Standard Processes (SDSP)



15 Manufacturing & Prototyping

- 15 Graphite Composite Panel Polishing Fixture
- 15 Material Gradients in Oxygen System Components Improve Safety
- 15 Ridge Waveguide Structures in Magnesium-Doped Lithium Niobate
- 16 Modifying Matrix Materials to Increase Wetting and Adhesion



17 Green Design

- 17 Lightweight Magnetic Cooler With a Reversible Circulator
- 17 The Invasive Species Forecasting System



19 Mechanics/Machinery

- 19 Method for Cleanly and Precisely Breaking Off a Rock Core Using a Radial Compressive Force
- 19 Praying Mantis Bending Core Breakoff and Retention Mechanism
- 20 Scoring Dawg Core Breakoff and Retention Mechanism
- 20 Rolling-Tooth Core Breakoff and Retention Mechanism
- 21 Vibration Isolation and Stabilization System for Spacecraft Exercise Treadmill Devices



23 Bio-Medical

- 23 Microgravity-Enhanced Stem Cell Selection
- 23 Diagnosis and Treatment of Neurological Disorders by Millimeter-Wave Stimulation



25 Physical Sciences

- 25 Passive Vaporizing Heat Sink
- 25 Remote Sensing and Quantization of Analog Sensors
- 25 Phase Retrieval for Radio Telescope and Antenna Control
- 26 Helium-Cooled Black Shroud for Subscale Cryogenic Testing



27 Information Sciences

- 27 Receive Mode Analysis and Design of Microstrip Reflectarrays
- 27 Chance-Constrained Guidance With Non-Convex Constraints

This document was prepared under the sponsorship of the National Aeronautics and Space Administration. Neither the United States Government nor any person acting on behalf of the United States Government assumes any liability resulting from the use of the information contained in this document, or warrants that such use will be free from privately owned rights.



Wind and Temperature Spectrometry of the Upper Atmosphere in Low-Earth Orbit

Multi-point measurements can enhance the capabilities of the GPS network, as well as other communication applications.

Goddard Space Flight Center, Greenbelt, Maryland

Wind and Temperature Spectrometry (WATS) is a new approach to measure the full wind vector, temperature, and relative densities of major neutral species in the Earth's thermosphere. The method uses an energy-angle spectrometer moving through the tenuous upper atmosphere to measure directly the angular and energy distributions of the air stream that enters the spectrometer. The angular distribution gives the direction of the total velocity of the air entering the spectrometer, and the energy distribution gives the magnitude of the total velocity. The wind velocity vector is uniquely determined since the measured total velocity depends on the wind vector and the orbiting velocity vector.

The orbiting spectrometer moves supersonically, Mach 8 or greater, through the air and must point within a few de-

grees of its orbital velocity vector (the ram direction). Pointing knowledge is critical; for example, pointing errors 0.1° lead to errors of about 10 m/s in the wind. The WATS method may also be applied without modification to measure the ion-drift vector, ion temperature, and relative ion densities of major ionic species in the ionosphere. In such an application it may be called IDTS: Ion-Drift Temperature Spectrometry.

A spectrometer-based coordinate system with one axis instantaneously pointing along the ram direction makes it possible to transform the Maxwellian velocity distribution of the air molecules to a Maxwellian energy-angle distribution for the molecular flux entering the spectrometer. This implementation of WATS is called the gas kinetic method (GKM) because it is applied to the case of the Maxwellian distribution.

The WATS method follows from the recognition that in a supersonic platform moving at 8,000 m/s, the measurement of small wind velocities in the air on the order of a few 100 m/s and less requires precise knowledge of the angle of incidence of the neutral atoms and molecules. The same is true for the case of ion-drift measurements. WATS also provides a general approach that can obtain non-equilibrium distributions as may exist in the upper regions of the thermosphere, above 500 km and into the exosphere. Finally, WATS serves as a mass spectrometer, with very low mass resolution of roughly 1 part in 3, but easily separating atomic oxygen from molecular nitrogen.

This work was done by Federico Herrero of Goddard Space Flight Center. Further information is contained in a TSP (see page 1). GSC-15753-1

Health Monitor for Multitasking, Safety-Critical, Real-Time Software

A single software module addresses many health management problems.

John F. Kennedy Space Center, Florida

Health Manager can detect "Bad Health" prior to a failure occurring by periodically monitoring the application software by looking for code corruption errors, and sanity-checking each critical data value prior to use. A processor's memory can fail and corrupt the software, or the software can accidentally write to the wrong address and overwrite the executing software. This innovation will continuously calculate a checksum of the software load to detect corrupted code. This will allow a system to detect a failure before it happens.

This innovation monitors each software task (thread) so that if any task reports "bad health," or does not report to

the Health Manager, the system is declared bad. The Health Manager reports overall system health to the outside world by outputting a square wave signal. If the square wave stops, this indicates that system health is bad or hung and cannot report. Either way, "bad health" can be detected, whether caused by an error, corrupted data, or a hung processor.

A separate Health Monitor Task is started and run periodically in a loop that starts and stops pending on a semaphore. Each monitored task registers with the Health Manager, which maintains a count for the task. The registering task must indicate if it will run more

or less often than the Health Manager. If the task runs more often than the Health Manager, the monitored task calls a health function that increments the count and verifies it did not go over max-count. When the periodic Health Manager runs, it verifies that the count did not go over the max-count and zeroes it. If the task runs less often than the Health Manager, the periodic Health Manager will increment the count. The monitored task zeroes the count, and both the Health Manager and monitored task verify that the count did not go over the max-count.

The Health Manager reports its system health status to the outside world by tog-

gling an output pin creating a square wave signal. If the system hangs completely prior to reporting its health status, the square wave is no longer generated. This absence of the square wave, whether intentional or because the Health Manager is hung, indicates bad health, analogous to a deadman switch. This is done by

creating a Health Manager Reporting Task, which loops and pends on a semaphore. A timer Interrupt Service Routine gives the semaphore that allows the Health Manager to run. When the Health Manager Reporting Task receives the semaphore, it reads the system health status. If the status is good, an output pin is

toggled. If the status is bad health, it latches the system's bad health variable so it can never switch back to good health and stops the square wave.

This work was done by Roger Zoerner of Kennedy Space Center. Further information is contained in a TSP (see page 1). KSC-12809

Stereo Imaging Miniature Endoscope

This endoscope can be used in minimally invasive surgery, in geological resource exploration, and in miniature analytical tools.

NASA's Jet Propulsion Laboratory, Pasadena, California

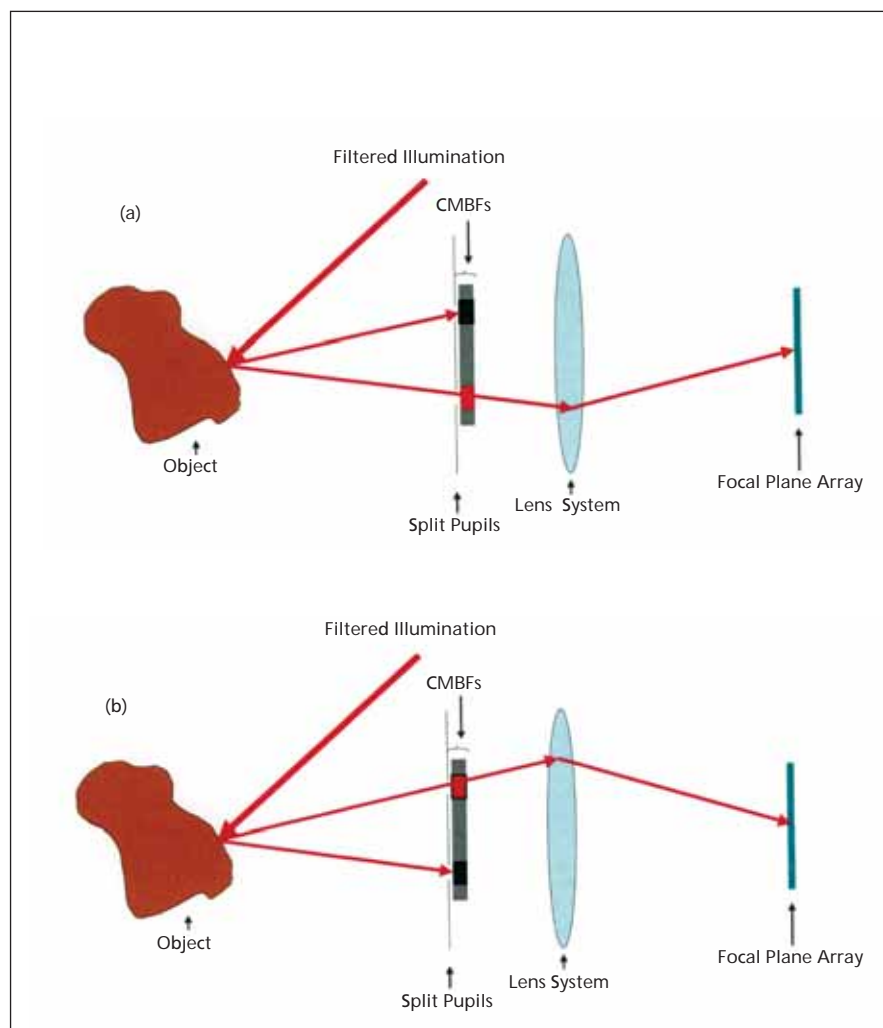
Stereo imaging requires two different perspectives of the same object and, traditionally, a pair of side-by-side cameras would be used but are not feasible for something as tiny as a less than 4-mm-diameter endoscope that could be used for minimally invasive surgeries or geoexploration through tiny fissures or bores. The proposed solution here is to employ a single lens, and a pair of conjugated, multiple-bandpass filters (CMBFs) to separate stereo images. When a CMBF is placed in front of each of the stereo channels, only one wavelength of the visible spectrum that falls within the passbands of the CMBF is transmitted through at a time when illuminated. Because the passbands are conjugated, only one of the two channels will see a particular wavelength. These time-multiplexed images are then mixed and reconstructed to display as stereo images.

The basic principle of stereo imaging involves an object that is illuminated at specific wavelengths, and a range of illumination wavelengths is time multiplexed. The light reflected from the object selectively passes through one of the two CMBFs integrated with two pupils separated by a baseline distance, and is focused onto the imaging plane through an objective lens. The passband range of CMBFs and the illumination wavelengths are synchronized such that each of the CMBFs allows transmission of only the alternate illumination wavelength bands. And the transmission bandwidths of CMBFs are complementary to each other, so that when one transmits, the other one blocks.

This can be clearly understood if the wavelength bands are divided broadly into red, green, and blue, then the illumination wavelengths contain two bands in red (R1, R2), two bands in green (G1, G2), and two bands in blue (B1, B2).

Therefore, when the objective is illuminated by R1, the reflected light enters through only the left-CMBF as the R1 band corresponds to the transmission window of the left CMBF at the left pupil. This is blocked by the right CMBF.

The transmitted band is focused on the focal plane array (FPA). Here, the FPA does not include color filter array (black and white); hence, the image sensors only measure light intensities. Similarly, when the object is illuminated by R2, it is



Schematic showing the principle of the **Stereo Imaging Endoscope** using CMBFs. (a) The first illumination band passes through the left CMBF to cast an image at the focal plane, but is blocked by the right CMBF. (b) The second illumination band passes through the right CMBF to cast an image at the focal plane, but is blocked by the left CMBF.

transmitted only through the right-CMBF and is blocked by the left-CMBF. This continues over other wavelength bands as well.

So, it can be seen that the image sensors at the focal plane are measuring light intensities of alternately transmitted light from the two CMBFs. At the end of one complete illumination cycle, six images will have been collected. Then the images from R1, G1, and B1 become the primary colors for the left side of the stereo image, and R2, G2, and B2 become that of the right side of

the stereo image. Two stereo images have been time-multiplexed on the same imaging chip. This intensity data is stored as an array from which the 3D stereoscopic color image is constructed by applying processing and reconstruction algorithms.

This work was done by Youngsam Bae, Harish Manohara, Victor E. White, and Kirill V. Shcheglov of Caltech and Hrayr Shahinian of Skull Base Institute for NASA's Jet Propulsion Laboratory. Further information is contained in a TSP (see page 1).

In accordance with Public Law 96-517, the contractor has elected to retain title to this invention. Inquiries concerning rights for its commercial use should be addressed to:

*Innovative Technology Assets Management
JPL*

Mail Stop 202-233

4800 Oak Grove Drive

Pasadena, CA 91109-8099

E-mail: iaoffice@jpl.nasa.gov

Refer to NPO-47420, volume and number of this NASA Tech Briefs issue, and the page number.

Early Oscillation Detection Technique for Hybrid DC/DC Converters

Potential users include commercial and military power supply manufacturers, and high-reliability electronic product companies.

Goddard Space Flight Center, Greenbelt, Maryland

Oscillation or instability is a situation that must be avoided for reliable hybrid DC/DC converters. A real-time electronics measurement technique was developed to detect catastrophic oscillations at early stages for hybrid DC/DC converters. It is capable of identifying low-level oscillation and determining the degree of the oscillation at a unique frequency for every individual model of the converters without disturbing their normal operations. This technique is specially developed for space-used hybrid DC/DC converters, but it is also suitable for most of commercial and military switching-mode power supplies.

This is a weak-electronic-signal detection technique to detect hybrid DC/DC converter oscillation presented as a specific noise signal at power input pins. It is based on principles of feedback control loop oscillation and RF signal modula-

tions, and is realized by using signal power spectral analysis. On the power spectrum, a channel power amplitude at characteristic frequency (CP_{cf}) and a channel power amplitude at switching frequency (CP_{sw}) are chosen as oscillation level indicators. If the converter is stable, the CP_{cf} is a very small pulse and the CP_{sw} is a larger, clear, single pulse. At early stage of oscillation, the CP_{cf} increases to a certain level and the CP_{sw} shows a small pair of sideband pulses around it. If the converter oscillates, the CP_{cf} reaches to a higher level and the CP_{sw} shows more high-level sideband pulses. A comprehensive stability index (CSI) is adopted as a quantitative measure to accurately assign a degree of stability to a specific DC/DC converter. The CSI is a ratio of normal and abnormal power spectral density, and can be calculated using specified and measured CP_{cf} and CP_{sw} data.

The novel and unique feature of this technique is the use of power channel amplitudes at characteristic frequency and switching frequency to evaluate stability and identify oscillations at an early stage without interfering with a DC/DC converter's normal operation. This technique eliminates the probing problem of a gain/phase margin method by connecting the power input to a spectral analyzer. Therefore, it is able to evaluate stability for all kinds of hybrid DC/DC converters with or without remote sense pins, and is suitable for real-time and in-circuit testing. This frequency-domain technique is more sensitive to detect oscillation at early stage than the time-domain method using an oscilloscope.

This work was done by Bright L. Wang of Goddard Space Flight Center. Further information is contained in a TSP (see page 1). GSC-15777-1

Parallel Wavefront Analysis for a 4D Interferometer

NASA's Jet Propulsion Laboratory, Pasadena, California

This software provides a programming interface for automating data collection with a PhaseCam interferometer from 4D Technology, and distributing the image-processing algorithm across a cluster of general-purpose computers.

Multiple instances of 4Sight (4D Technology's proprietary software) run on a

networked cluster of computers. Each connects to a single server (the controller) and waits for instructions. The controller directs the interferometer to several images, then assigns each image to a different computer for processing. When the image processing is finished, the server directs one of the computers

to collate and combine the processed images, saving the resulting measurement in a file on a disk.

The available software captures approximately 100 images and analyzes them immediately. This software separates the capture and analysis processes, so that analysis can be done

at a different time and faster by running the algorithm in parallel across several processors.

The PhaseCam family of interferometers can measure an optical system in milliseconds, but it takes many seconds to process the data so that it is usable. In characterizing an adaptive optics system, like the next generation of astronomical observatories, thousands of measure-

ments are required, and the processing time quickly becomes excessive.

A programming interface distributes data processing for a PhaseCam interferometer across a Windows computing cluster. A scriptable controller program coordinates data acquisition from the interferometer, storage on networked hard disks, and parallel processing. Idle time of the interferometer is minimized.

This architecture is implemented in Python and JavaScript, and may be altered to fit a customer's needs.

This work was done by Shanti R. Rao of Caltech for NASA's Jet Propulsion Laboratory. For more information, contact iaoffice@jpl.nasa.gov.

This software is available for commercial licensing. Please contact Daniel Broderick of the California Institute of Technology at danielb@caltech.edu. Refer to NPO-47384.



Schottky Heterodyne Receivers With Full Waveguide Bandwidth

New receivers are designed for high-resolution spectroscopic studies.

Goddard Space Flight Center, Greenbelt, Maryland

Compact THz receivers with broad bandwidth and low noise have been developed for the frequency range from 100 GHz to 1 THz. These receivers meet the requirements for high-resolution spectroscopic studies of planetary atmospheres (including the Earth's) from spacecraft, as well as airborne and balloon platforms. The ongoing research is significant not only for the development of Schottky mixers, but also for the creation of a receiver system, including the LO chain.

The new receivers meet the goals of high sensitivity, compact size, low total power requirement, and operation across complete waveguide bands. The exceptional performance makes these receivers ideal for the broader range of scientific and commercial applications. These include the extension of sophisticated test and measurement equipment to 1 THz and the development of low-cost imaging systems for security applications and industrial process monitoring. As a particular example, a WR-1.9SHM

(400–600 GHz) has been developed (see Figure 1), with state-of-the-art noise temperature ranging from 1,000–1,800 K (DSB) over the full waveguide band. Also, a Vector Network Analyzer extender has been developed (see Figure 2) for the WR1.5 waveguide band (500–750 GHz) with 100-dB dynamic range.

This work was done by Jeffrey Hesler and Thomas Crowe of Virginia Diodes, Inc. for Goddard Space Flight Center. Further information is contained in a TSP (see page 1). GSC-15798-1

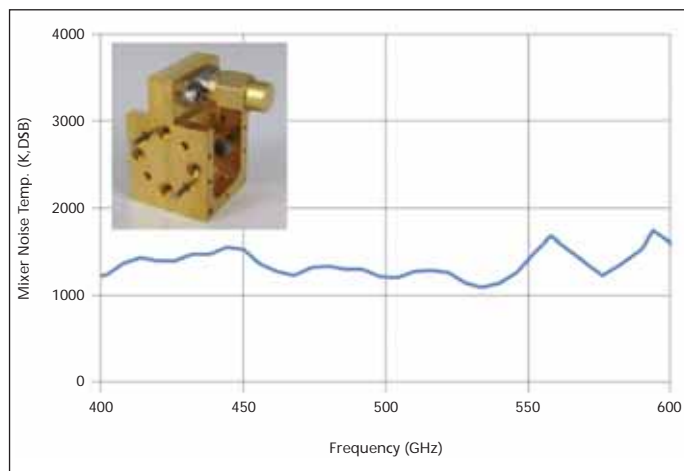


Figure 1. Measured Performance of a WR-1.9 (400–600 GHz) subharmonic mixer (shown in inset).

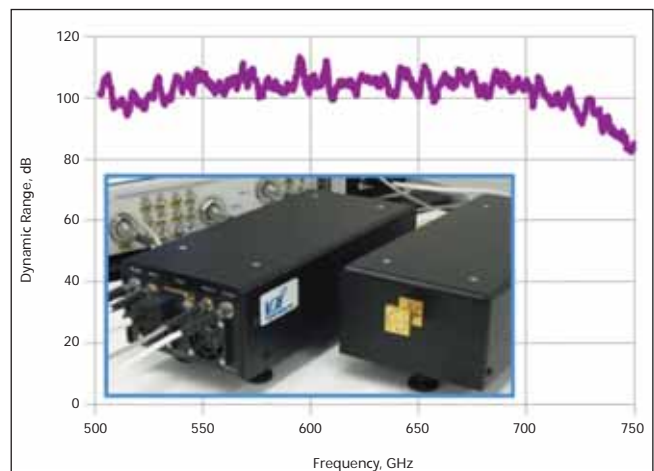


Figure 2. Measured Dynamic Range of a VDI WR-1.5 (500–750 GHz) VNA frequency extender module.

Carbon Nanofiber-Based, High-Frequency, High-Q, Miniaturized Mechanical Resonators

These miniature resonators can be used in portable electronics, communications systems, and other wireless systems.

NASA's Jet Propulsion Laboratory, Pasadena, California

High Q resonators are a critical component of stable, low-noise communication systems, radar, and precise timing applications such as atomic clocks. In electronic resonators based on Si integrated circuits, resistive losses increase as a result of the continued reduction in device dimensions, which decreases their Q values. On the other hand, due to the

mechanical construct of bulk acoustic wave (BAW) and surface acoustic wave (SAW) resonators, such loss mechanisms are absent, enabling higher Q-values for both BAW and SAW resonators compared to their electronic counterparts. The other advantages of mechanical resonators are their inherently higher radiation tolerance, a factor that makes them

attractive for NASA's extreme environment planetary missions, for example to the Jovian environments where the radiation doses are at hostile levels. Despite these advantages, both BAW and SAW resonators suffer from low resonant frequencies and they are also physically large, which precludes their integration into miniaturized electronic systems.

Because there is a need to move the resonant frequency of oscillators to the order of gigahertz, new technologies and materials are being investigated that will make performance at those frequencies attainable. By moving to nanoscale structures, in this case vertically oriented, cantilevered carbon nanotubes (CNTs), that have larger aspect ratios (length/thickness) and extremely high elastic moduli, it is possible to overcome the two disadvantages of both bulk acoustic wave (BAW) and surface acoustic wave (SAW) resonators.

Nano-electro-mechanical systems (NEMS) that utilize high aspect ratio nanomaterials exhibiting high elastic moduli (e.g., carbon-based nanomaterials) benefit from high Qs, operate at high frequency, and have small force constants that translate to high responsiveness that results in improved sensitivity, lower power consumption, and improved tunability. NEMS resonators have recently been demonstrated using top-down, lithographically fabricated approaches to form cantilever or bridge-type structures. Top-down approaches, however, rely on complicated and expensive e-beam lithography, and often require a release mechanism. Resonance effects in structures synthesized using bottom-up approaches have also recently been reported based on carbon nanotubes, but such approaches have relied on a planar two-dimensional (2D) geometry. In this innovation, vertically aligned tubes synthesized using a bot-

tom-up approach have been considered, where the vertical orientation of the tubes has the potential to increase integration density even further.

The simulation of a vertically oriented, cantilevered carbon nanotube was performed using COMSOL Multiphysics, a finite element simulation package. All simulations were performed in a 2D geometry that provided consistent results and minimized computational complexity. The simulations assumed a vertically oriented, cantilevered nanotube of uniform density (1.5 g/cm^3). An elastic modulus was assumed to be 600 GPa, relative permittivity of the nanotube was assumed to be 5.0, and Poisson's ratio was assumed to be 0.2. It should be noted that the relative permittivity and Poisson's ratio for the nanotubes of interest are not known accurately. However, as in previous simulations, the relative permittivity and Poisson's ratios were treated as weak variables in the simulation, and no significant changes were recognized when these variables were varied.

Of interest in the simulations of a CNT resonator were the structural strain and deflection of the nanotube, and the electrostatic interactions between the nanotube and nanomanipulator probe. Structural boundary conditions were arranged such that the exposed lengths and tip of the nanotube were allowed to move freely while all other surfaces were held fixed (including the nanotube base). These conditions simulated a

fixed, cantilevered beam in a domain adjacent to a nanomanipulator probe of infinite elastic modulus. Electrostatic boundary conditions were chosen such that the nanotube was grounded, an AC voltage with DC bias was applied to the surface of the nanoprobe adjacent to the nanotube, and all other boundaries in the system were selected such that no electrical charge exists on, or outside of, those surfaces. The solution domain was simulated as a vacuum. Preliminary experiments have suggested that electro-mechanical coupling can occur between a scanning electron microscope (SEM) beam and a vertically oriented, cantilever carbon nanofiber (CNF) causing the CNF to mechanically resonate with displacements two or three times larger than the tube diameters.

This work was done by Anupama B. Kaul and Larry W. Epp of Caltech and Leif Bagge of the University of Texas for NASA's Jet Propulsion Laboratory. For more information, contact iaoffice@jpl.nasa.gov.

In accordance with Public Law 96-517, the contractor has elected to retain title to this invention. Inquiries concerning rights for its commercial use should be addressed to:

*Innovative Technology Assets Management
JPL*

*Mail Stop 202-233
4800 Oak Grove Drive
Pasadena, CA 91109-8099*

E-mail: iaoffice@jpl.nasa.gov

Refer to NPO-47238, volume and number of this NASA Tech Briefs issue, and the page number.

Ultracapacitor-Based Uninterrupted Power Supply System

This technology provides essential backup power, increases safety, and reduces environmental impact.

John H. Glenn Research Center, Cleveland, Ohio

The ultracapacitor-based uninterrupted power supply (UPS) system enhances system reliability; reduces life-of-system, maintenance, and downtime costs; and greatly reduces environmental impact when compared to conventional UPS energy storage systems. This design provides power when required and absorbs power when required to smooth the system load and also has excellent low-temperature performance. The UPS used during hardware tests at Glenn is an efficient, compact, maintenance-free, rack-mount, pure sine-wave inverter unit.

The UPS provides a continuous output power up to 1,700 W with a surge rating of 1,870 W for up to one minute at a nominal output voltage of 115 VAC. The ultracapacitor energy storage system tested in conjunction with the UPS is rated at 5.8 F. This is a bank of ten symmetric ultracapacitor modules.

Each module is actively balanced using a linear voltage balancing technique in which the cell-to-cell leakage is dependent upon the imbalance of the individual cells. The ultracapacitors are charged by a DC power supply, which can provide up to 300 VDC at 4 A. A

constant-voltage, constant-current power supply was selected for this application. The long life of ultracapacitors greatly enhances system reliability, which is significant in critical applications such as medical power systems and space power systems. The energy storage system can usually last longer than the application, given its 20-year life span. This means that the ultracapacitors will probably never need to be replaced and disposed of, whereas batteries require frequent replacement and disposal. The charge-discharge efficiency of rechargeable batteries is ap-

proximately 50 percent, and after some hundreds of charges and discharges, they must be replaced. The charge-discharge efficiency of ultracapacitors exceeds 90 percent, and can accept more than a million charges and discharges. Thus, there is a significant energy savings through the efficiency improvement, and there is far less downtime for applications and labor involved in replacing an ultracapacitor versus batter-

ies. Also, the lengthy lifespan of this design would greatly reduce the disposal problems posed by lead acid, nickel cadmium, lithium, and nickel metal hydride batteries.

This innovation is recyclable by nature, which further reduces system costs. The disposal of ultracapacitors is simple, as they are constructed of non-hazardous components. They are also safer than batteries in that they can be easily dis-

charged, and left indefinitely in a safe, discharged state where batteries cannot.

This work was done by Dennis J. Eichenberg for Glenn Research Center. Further information is contained in a TSP (see page 1).

Inquiries concerning rights for the commercial use of this invention should be addressed to NASA Glenn Research Center, Innovative Partnerships Office, Attn: Steven Fedor, Mail Stop 4-8, 21000 Brookpark Road, Cleveland, Ohio 44135. Refer to LEW-18649-1.

Coaxial Cables for Martian Extreme Temperature Environments

NASA's Jet Propulsion Laboratory, Pasadena, California

Work was conducted to validate the use of the rover external flexible coaxial cabling for space under the extreme environments to be encountered during the Mars Science Laboratory (MSL) mission. The antennas must survive all ground operations plus the nominal 670-Martian-day mission that includes summer and winter seasons of the Mars environment.

Successful development of processes established coaxial cable hardware fatigue limits, which were well beyond the expected in-flight exposures. In keeping with traditional qualification philoso-

phy, this was accomplished by subjecting flight-representative coaxial cables to temperature cycling of the same depth as expected in-flight, but for three times the expected number of in-flight thermal cycles.

Insertion loss and return loss tests were performed on the coaxial cables during the thermal chamber breaks. A vector network analyzer was calibrated and operated over the operational frequency range 7.145 to 8.450 GHz. Even though some of the exposed cables function only at UHF frequencies (approximately 400 MHz), the testing was

more sensitive, and extending the test range down to 400 MHz would have cost frequency resolution.

The Gore flexible coaxial cables, which were the subject of these tests, proved to be robust and displayed no sign of degradation due to the 3X exposure to the punishing Mars surface operations cycles.

This work was done by Rajeshuni Ramesham, Wayne L. Harvey, Sam Valas, and Michael C. Tsai of Caltech for NASA's Jet Propulsion Laboratory. For more information, contact iaoffice@jpl.nasa.gov. NPO-47452

Using Spare Logic Resources To Create Dynamic Test Points

Goddard Space Flight Center, Greenbelt, Maryland

A technique has been devised to enable creation of a dynamic set of test points in an embedded digital electronic system. As a result, electronics contained in an application specific circuit [e.g., gate array, field programmable gate array (FPGA)] can be internally "probed," even when contained in a closed housing during all phases of test.

In the present technique, the test points are not fixed and limited to a small number; the number of test points

can vastly exceed the number of buffers or pins, resulting in a compact footprint. Test points are selected by means of spare logic resources within the ASIC(s) and/or FPGA(s). A register is programmed with a command, which is used to select the signals that are sent off-chip and out of the housing for monitoring by test engineers and external test equipment.

The register can be commanded by any suitable means: for example, it

could be commanded through a command port that would normally be used in the operation of the system. In the original application of the technique, commanding of the register is performed via a MIL-STD-1553B communication subsystem.

This work was done by Richard Katz and Igor Kleyner of Goddard Space Flight Center. Further information is contained in a TSP (see page 1). GSC-15490-1



Autonomous Coordination of Science Observations Using Multiple Spacecraft

This software provides capabilities for autonomous cross-cueing and coordinated observations between multiple orbital and landed assets. Previous work has been done in re-tasking a single Earth orbiter or a Mars rover in response to that craft detecting a science event. This work enables multiple spacecraft to communicate (over a network designed for deep-space communications) and autonomously coordinate the characterization of such a science event.

This work investigates a new paradigm of space science campaigns where opportunistic science observations are autonomously coordinated among multiple spacecraft. In this paradigm, opportunistic science detections can be cued by multiple assets where a second asset is requested to take additional observations characterizing the identified surface feature or event. To support this new paradigm, an autonomous science system for multiple spacecraft assets was integrated with the Interplanetary Network DTN (Delay Tolerant Network) to provide communication between spacecraft assets.

This technology enables new mission concepts that are not feasible with current technology. The ability to rapidly coordinate activities across spacecraft without requiring ground in the loop enables rapid reaction to dynamic events across platforms, such as a survey instrument followed by a targeted high-resolution instrument, as well as regular simultaneous observations.

This work was done by Tara A. Estlin, Steve A. Chien, Rebecca Castano, Daniel M. Gaines, Joshua R. Doubleday, Joshua B. Schoolcraft, Amalaye Oyake, Ashton G. Vaughs, and Jordan L. Torgerson of Caltech and Charles de Granville for NASA's Jet Propulsion Laboratory. For more information, contact iaoffice@jpl.nasa.gov.

This software is available for commercial licensing. Please contact Daniel Broderick of the California Institute of Technology at danielb@caltech.edu. Refer to NPO-47398.

Autonomous Phase Retrieval Calibration

The Palomar Adaptive Optics System actively corrects for changing aberrations

in light due to atmospheric turbulence. However, the underlying internal static error is unknown and uncorrected by this process. The dedicated wavefront sensor device necessarily lies along a different path than the science camera, and, therefore, doesn't measure the true errors along the path leading to the final detected imagery. This is a standard problem in adaptive optics (AO) called "non-common path error."

The previous method of calibrating this error consisted of manually applying different polynomial shapes (via actuator voltages) at different magnitudes onto the deformable mirror and noting if the final image quality had improved or deteriorated, before moving onto the next polynomial mode. This is a limited, time-consuming, and subjective process, and structural and environmental changes over time necessitate a new calibration over a period of months.

The Autonomous Phase Retrieval Calibration (APRC) software suite performs automated sensing and correction iterations to calibrate the Palomar AO system to levels that were previously unreachable. APRC controls several movable components inside the AO system to collect the required data, automatically processes data using an adaptive phase retrieval algorithm, and automatically calculates new sets of actuator voltage commands for the deformable mirror. APRC manages and preserves all essential data during this process.

The APRC software calculates the true wavefront error of the full optical system, then uses the existing AO system deformable mirror (DM) to correct the detected error. This provides a significant leap in performance by precisely correcting what were once "un-calibratable" errors. Furthermore, the corrective pattern found by this process serves as the underlying nominal shape of the DM, upon which the adaptive corrections for atmospheric turbulence are based.

This work was done by Siddarayappa A. Bikkannavar, Catherine M. O'Hara, and Mitchell Troy of Caltech for NASA's Jet Propulsion Laboratory. Further information is contained in a TSP (see page 1).

This software is available for commercial licensing. Please contact Daniel Broderick of the California Institute of Technology at danielb@caltech.edu. Refer to NPO-47270.

EOS MLS Level 1B Data Processing Software, Version 3

This software is an improvement on Version 2, which was described in "EOS MLS Level 1B Data Processing, Version 2.2," *NASA Tech Briefs*, Vol. 33, No. 5 (May 2009), p. 34. It accepts the EOS MLS Level 0 science/engineering data, and the EOS Aura spacecraft ephemeris/attitude data, and produces calibrated instrument radiances and associated engineering and diagnostic data. This version makes the code more robust, improves calibration, provides more diagnostics outputs, defines the Galactic core more finely, and fixes the equator crossing.

The Level 1 processing software manages several different tasks. It qualifies each data quantity using instrument configuration and checksum data, as well as data transmission quality flags. Statistical tests are applied for data quality and reasonableness. The instrument engineering data (e.g., voltages, currents, temperatures, and encoder angles) is calibrated by the software, and the filter channel space reference measurements are interpolated onto the times of each limb measurement with the interpolates being differenced from the measurements. Filter channel calibration target measurements are interpolated onto the times of each limb measurement, and are used to compute radiometric gain. The total signal power is determined and analyzed by each digital autocorrelator spectrometer (DACS) during each data integration. The software converts each DACS data integration from an autocorrelation measurement in the time domain into a spectral measurement in the frequency domain, and estimates separately the spectrally, smoothly varying and spectrally averaged components of the limb port signal arising from antenna emission and scattering effects. Limb radiances are also calibrated.

The radiance at the limb port of the radiometer module is computed, including non-atmospheric radiance contributions from antenna emission and scattering. It is the task of the retrieval/forward model software (Level 2) to compute the atmospheric component of the limb radiation reaching this interface. It is necessitated by the greatly increased bandwidth of EOS MLS radiometers, and the

double-sideband nature of most measurements. Estimates of the random component of uncertainty (noise) on each limb radiance are also determined. Spacecraft inertial pointing and star tracker data are combined with spacecraft and GHz antenna structural/thermal data and scan mechanism encoder data to estimate the boresight angles for each radiometer. The software collects and generates ancillary data (e.g., tangent point location, local solar time, local solar zenith angle, flags for bright objects in the field of view) that are needed in Level 2 processing. A log file is produced that summarizes instrument performance and outputs.

This work was done by Vincent S. Perun, Robert F. Jarnot, Paul A. Wagner, Richard E. Cofield IV, and Honghanh T. Nguyen of Caltech and Christina Vuu of Raytheon for NASA's Jet Propulsion Laboratory. For more information, contact iaoffice@jpl.nasa.gov.

This software is available for commercial licensing. Please contact Daniel Broderick of the California Institute of Technology at danielb@caltech.edu. Refer to NPO-47219.

Cassini Tour Atlas Automated Generation

During the Cassini spacecraft's cruise phase and nominal mission, the Cassini Science Planning Team developed and maintained an online database of geometric and timing information called the Cassini Tour Atlas. The Tour Atlas consisted of several hundreds of megabytes of EVENTS mission planning software outputs, tables, plots, and images used by mission scientists for observation planning. Each time the nominal

mission trajectory was altered or tweaked, a new Tour Atlas had to be regenerated manually.

In the early phases of Cassini's Equinox Mission planning, an *a priori* estimate suggested that mission tour designers would develop approximately 30 candidate tours within a short period of time. So that Cassini scientists could properly analyze the science opportunities in each candidate tour quickly and thoroughly so that the optimal series of orbits for science return could be selected, a separate Tour Atlas was required for each trajectory.

The task of manually generating the number of trajectory analyses in the allotted time would have been impossible, so the entire task was automated using code written in five different programming languages. This software automates the generation of the Cassini Tour Atlas database. It performs with one UNIX command what previously took a day or two of human labor.

This work was done by Kevin R. Grazier, Chris Roumeliotis, and Robert D. Lange of Caltech for NASA's Jet Propulsion Laboratory. For more information, contact iaoffice@jpl.nasa.gov.

This software is available for commercial licensing. Please contact Daniel Broderick of the California Institute of Technology at danielb@caltech.edu. Refer to NPO-47282.

Software Development Standard Processes (SDSP)

A JPL-created set of standard processes is to be used throughout the lifecycle of software development. These SDSPs cover a range of activities, from management and engineering activities,

to assurance and support activities. These processes must be applied to software tasks per a prescribed set of procedures. JPL's Software Quality Improvement Project is currently working at the behest of the JPL Software Process Owner to ensure that all applicable software tasks follow these procedures.

The SDSPs are captured as a set of 22 standards in JPL's software process domain. They were developed in-house at JPL by a number of Subject Matter Experts (SMEs) residing primarily within the Engineering and Science Directorate, but also from the Business Operations Directorate and Safety and Mission Success Directorate. These practices include not only currently performed best practices, but also JPL-desired future practices in key thrust areas like software architecting and software reuse analysis. Additionally, these SDSPs conform to many standards and requirements to which JPL projects are beholden.

This work was done by Milton L. Lavin, James J. Wang, Ronald Morillo, John T. Mayer, Barzia Jamshidian Tehrani, Kenneth J. Shimizu, Belinda M. Wilkinson, Jairus M. Hihn, Rosana B. Borgen, Kenneth N. Meyer, Kathleen A. Crean, George C. Rinker, Thomas P. Smith, Karen T. Lum, Robert A. Hanna, Daniel E. Erickson, Edward B. Gamble Jr., Scott C. Morgan, Michael G. Kelsay, Brian J. Newport, Scott A. Lewicki, Jeane G. Stipanuk, Tonja M. Cooper, and Leila Meshkat of Caltech for NASA's Jet Propulsion Laboratory. Further information is contained in a TSP (see page 1).

This software is available for commercial licensing. Please contact Daniel Broderick of the California Institute of Technology at danielb@caltech.edu. Refer to NPO-47301.



Graphite Composite Panel Polishing Fixture

Composite fixture eliminates problems that may be caused by those made from aluminum.

Goddard Space Flight Center, Greenbelt, Maryland

The use of high-strength, lightweight composites for the fixture is the novel feature of this innovation. The main advantage is the light weight and high stiffness-to-mass ratio relative to aluminum.

Meter-class optics require support during the grinding/polishing process with large tools. The use of aluminum as a polishing fixture is standard, with pitch providing a compliant layer to allow support without deformation. Unfortunately, with meter-scale optics, a meter-scale fixture weighs over 120 lb (≈ 55 kg) and may distort the optics being fabricated by loading the mirror and/or tool used in fabrication. The use of composite structures that are lightweight yet stiff allows standard techniques to be used while providing for a decrease in fixture weight by almost 70 percent.

Mounts classically used to support large mirrors during fabrication are especially heavy and difficult to handle. The mount must be especially stiff to avoid deformation during the optical fabrication process, where a very large and heavy lap often can distort the mount and optic being fabricated. If the optic is placed on top of the lapping tool, the weight of the optic and the fixture can distort the lap. Fixtures to support the mirror during fabrication are often very large plates of aluminum, often 2 in. (≈ 5 cm) or more in thickness and weight upwards of 150 lb (≈ 68 kg). With the addition of a backing material such as pitch and the mirror itself, the assembly can often weigh over 250 lb (≈ 113 kg) for a meter-class optic.

This innovation is the use of a lightweight graphite panel with an aluminum honeycomb core for use as the polishing fixture. These materials have been used

in the aerospace industry as structural members due to their light weight and high stiffness. The grinding polishing fixture consists of the graphite composite panel, fittings, and fixtures to allow interface to the polishing machine, and introduction of pitch buttons to support the optic under fabrication. In its operation, the grinding polishing fixture acts as a reaction structure to the polishing tool. It must be stiff enough to avoid imparting a distorted shape to the optic under fabrication and light enough to avoid self-deflection. The fixture must also withstand significant tangential loads from the polishing machine during operations.

This work was done by John Hagopian, Carl Strojny, and Jason Budinoff of Goddard Space Flight Center. Further information is contained in a TSP (see page 1). GSC-15911-1

Material Gradients in Oxygen System Components Improve Safety

Lyndon B. Johnson Space Center, Houston, Texas

Oxygen system components fabricated by Laser Engineered Net Shaping™ (LENS™) could result in improved safety and performance. LENS™ is a near-net shape manufacturing process fusing powdered materials injected into a laser beam. Parts can be fabricated with a variety of elemental metals, alloys, and nonmetallic materials without the use of a mold. The LENS™

process allows the injected materials to be varied throughout a single workpiece. Hence, surfaces exposed to oxygen could be constructed of an oxygen-compatible material while the remainder of the part could be one chosen for strength or reduced weight. Unlike conventional coating applications, a compositional gradient would exist between the two materials, so no abrupt

material boundary exists. Without an interface between dissimilar materials, there is less tendency for chipping or cracking associated with thermal-expansion mismatches.

This work was done by Bradley S. Forsyth of Honeywell Technology Solutions, Inc., for Johnson Space Center. For further information, contact the JSC Innovation Partnerships Office at (281) 483-3809. MSC-23166-1

Ridge Waveguide Structures in Magnesium-Doped Lithium Niobate

Goddard Space Flight Center, Greenbelt, Maryland

This work proposes to establish the feasibility of fabricating isolated ridge waveguides in 5% MgO:LN. Ridge waveguides in MgO:LN will significantly improve power handling and conversion ef-

iciency, increase photonic component integration, and be well suited to space-based applications. The key innovation in this effort is to combine recently available large, high-photorefractive-damage-

threshold, z-cut 5% MgO:LN with novel ridge fabrication techniques to achieve high-optical power, low-cost, high-volume manufacturing of frequency conversion structures. The proposed ridge

waveguide structure should maintain the characteristics of the periodically poled bulk substrate, allowing for the efficient frequency conversion typical of waveguides and the high optical damage threshold and long lifetimes typical of the 5% doped bulk substrate. The low cost and large area of 5% MgO:LN wafers, and the improved performance of the proposed ridge waveguide structure, will enhance existing measurement capabilities as well as reduce the resources required to achieve high-performance specifications.

The purpose of the ridge waveguides in MgO:LN is to provide platform tech-

nology that will improve optical power handling and conversion efficiency compared to existing waveguide technology. The proposed ridge waveguide is produced using standard microfabrication techniques. The approach is enabled by recent advances in inductively coupled plasma etchers and chemical mechanical planarization techniques. In conjunction with wafer bonding, this fabrication methodology can be used to create arbitrarily shaped waveguides allowing complex optical circuits to be engineered in nonlinear optical materials such as magnesium doped lithium niobate. Researchers

here have identified NLO (nonlinear optical) ridge waveguide structures as having suitable value to be the leading frequency conversion structures. Its value is based on having the low-cost fabrication necessary to satisfy the challenging pricing requirements as well as achieve the power handling and other specifications in a suitably compact package.

This work was done by Phillip Himmer of Montana State University and Philip Battle, William Suckow, and Greg Switzer of AdvR Inc. for Goddard Space Flight Center. Further information is contained in a TSP (see page 1). GSC-16031-1

Modifying Matrix Materials to Increase Wetting and Adhesion

Improvements are achieved at lower cost and without degradation of fibers.

Marshall Space Flight Center, Alabama

In an alternative approach to increasing the degrees of wetting and adhesion between the fiber and matrix components of organic-fiber/polymer matrix composite materials, the matrix resins are modified. Heretofore, it has been common practice to modify the fibers rather than the matrices: The fibers are modified by chemical and/or physical surface treatments prior to combining the fibers with matrix resins — an approach that entails considerable expense and usually results in degradation (typically, weakening) of fibers.

The alternative approach of modifying the matrix resins does not entail degradation of fibers, and affords opportunities for improving the mechanical properties of the fiber composites.

The alternative approach is more cost-effective, not only because it eliminates expensive fiber-surface treatments but also because it does not entail changes in procedures for manufacturing conventional composite-material structures.

The alternative approach is best described by citing an example of its application to a composite of ultra-high-molecular-weight polyethylene (UHMWPE) fibers in an epoxy matrix. The epoxy matrix was modified to a chemically reactive, polarized epoxy nano-matrix to increase the degrees of wetting and adhesion between the fibers and the matrix. The modification was effected by incorporating a small proportion (0.3 weight percent) of reactive graphitic nanofibers produced from functional-

ized nanofibers into the epoxy matrix resin prior to combining the resin with the UHMWPE fibers. The resulting increase in fiber/matrix adhesion manifested itself in several test results, notably including an increase of 25 percent in the maximum fiber pullout force and an increase of 60–65 percent in fiber pullout energy. In addition, it was conjectured that the functionalized nanofibers became involved in the cross linking reaction of the epoxy resin, with resultant enhancement of the mechanical properties and lower viscosity of the matrix.

This work was done by Katie Zhong of North Dakota State University for Marshall Space Flight Center. For further information, contact Sammy Nabors, MSFC Commercialization Assistance Lead, at sammy.a.nabors@nasa.gov. Refer to MFS-32665-1



Lightweight Magnetic Cooler With a Reversible Circulator

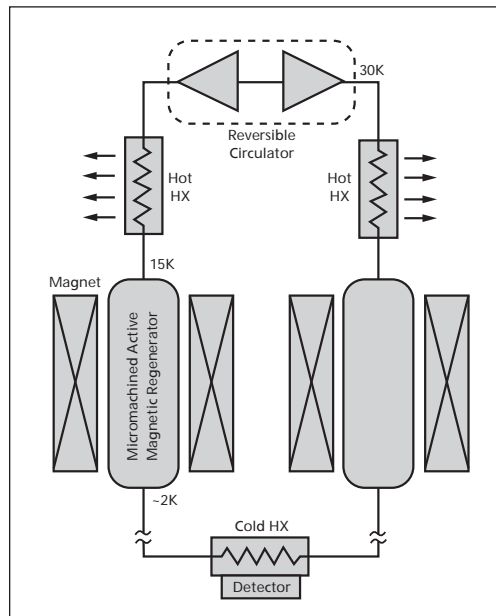
This lightweight design features relatively high efficiency.

Goddard Space Flight Center, Greenbelt, Maryland

A design of a highly efficient and lightweight space magnetic cooler has been developed that can continuously provide remote/distributed cooling at temperatures in the range of 2 K with a heat sink at about 15 K. The innovative design uses a cryogenic circulator that enables the cooler to operate at a high cycle frequency to achieve a large cooling capacity. The ability to provide remote/distributed cooling not only allows flexible integration with a payload and spacecraft, but also reduces the mass of the magnetic shields needed.

The active magnetic regenerative refrigerator (AMRR) system is shown in the figure. This design mainly consists of two identical magnetic regenerators surrounded by their superconducting magnets and a reversible circulator. Each regenerator also has a heat exchanger at its warm end to reject the magnetization heat to the heat sink, and the two regenerators share a cold-end heat exchanger to absorb heat from a cooling target.

The circulator controls the flow direction, which cycles in concert with the magnetic fields, to facilitate heat transfer. Helium enters the hot end of the demagnetized column, is cooled by the refrigerant, and passes into the cold-end heat exchanger to absorb heat. The helium then enters the cold end of the magnetized column, absorbing heat



System Schematic of a Magnetic Cooler with a reversible circulator. (Note: HX is heat exchanger)

from the refrigerant, and enters the hot-end heat exchanger to reject the magnetization heat. The efficient heat transfer in the AMRR allows the system to operate at a relatively short cycle period to achieve a large cooling power.

The key mechanical components in the magnetic cooler are the reversible circulator and the magnetic regenerators. The circulator uses non-contacting, self-acting gas bearings and clearance

seals to achieve long life and vibration-free operation. There are no valves or mechanical wear in this circulator, so the reliability is predicted to be very high. The magnetic regenerator employs a structured bed configuration. The core consists of a stack of thin GGG disks alternating with thin polymer insulating films. The structured bed reduces flow resistance in the regenerator and therefore the pumping work by the cryogenic circulator.

This magnetic cooler will enable cryogenic detectors for sensing infrared, x-ray, gamma-ray, and submillimeter radiation in future science satellites, as well as the detector systems in the Constellation-X (Con-X) and the Single Aperture Far-Infrared observatory (SAFIR). Scientific applications for this innovation include cooling for x-ray microcalorimeter spectrometers used for microanalysis, cryogenic particle detectors, and superconducting tunnel junction detectors for biomolecule mass spectrometry. The cooler can be scaled to provide very large cooling capacities at very low temperatures, ideal for liquid helium and liquid hydrogen productions.

This work was done by Weibo Chen and John McCormick of Creare, Inc. for Goddard Space Flight Center. Further information is contained in a TSP (see page 1). GSC-15410-1

The Invasive Species Forecasting System

Applications built using the Invasive Species Forecasting System help natural resource managers model habitat suitability for non-native, invasive plants.

Goddard Space Flight Center, Greenbelt, Maryland

The Invasive Species Forecasting System (ISFS) provides computational support for the generic work processes found in many regional-scale ecosystem modeling applications. Decision support tools built using ISFS allow a user to load

point occurrence field sample data for a plant species of interest and quickly generate habitat suitability maps for geographic regions of management concern, such as a national park, monument, forest, or refuge. This type

of decision product helps resource managers plan invasive species protection, monitoring, and control strategies for the lands they manage. Until now, scientists and resource managers have lacked the data-assembly and computing capa-

bilities to produce these maps quickly and cost efficiently.

ISFS focuses on regional-scale habitat suitability modeling for invasive terrestrial plants. ISFS's component architecture emphasizes simplicity and adaptability. Its core services can be easily adapted to produce model-based decision support tools tailored to particular parks, monuments, forests, refuges, and related management units. ISFS can be used to build standalone run-time tools that require no connection to the Internet, as well as fully Internet-based decision support applications.

ISFS provides the core data structures, operating system interfaces, network interfaces, and inter-component constraints comprising the canonical workflow for habitat suitability modeling. The predictors, analysis methods, and geographic extents involved in any particular model run are elements of the user space and arbitrarily configurable by the user. ISFS provides small, lightweight, readily hardened core components of general utility. These components can be adapted to unanticipated uses, are tailorable, and require at most a loosely coupled, non-proprietary connection to the Web. Users

can invoke capabilities from a command line; programmers can integrate ISFS's core components into more complex systems and services. Taken together, these features enable a degree of decentralization and distributed ownership that have helped other types of scientific information services succeed in recent years.

This work was done by John Schnase of Goddard Space Flight Center, Neal Most and Roger Gill of INNOVIM, and Peter Ma of Sigma Space Corporation. For further information, contact the Goddard Innovative Partnerships Office at (301) 286-5810. GSC-15714-1/61-7-1.



Method for Cleanly and Precisely Breaking Off a Rock Core Using a Radial Compressive Force

This technique can be used by civil engineers in rock, ground, and concrete coring and sampling.

NASA's Jet Propulsion Laboratory, Pasadena, California

The Mars Sample Return mission has the goal to drill, break off, and retain rock core samples. After some results gained from rock core mechanics testing, the realization that scoring teeth would cleanly break off the core after only a few millimeters of penetration, and noting that rocks are weak in tension, the idea was developed to use symmetric wedging teeth in compression to weaken and then break the core at the contact plane. This concept was developed as a response to the break-off and retention requirements.

The wedges wrap around the estimated average diameter of the core to

get as many contact locations as possible, and are then pushed inward, radially, through the core towards one another. This starts a crack and begins to apply opposing forces inside the core to propagate the crack across the plane of contact.

The advantage is in the simplicity. Only two teeth are needed to break five varieties of Mars-like rock cores with limited penetration and reasonable forces. Its major advantage is that it does not require any length of rock to be attached to the parent in order to break the core at the desired location. Test data shows that some rocks break off on

their own into segments or break off into discs. This idea would grab and retain a disc, push some discs upward and others out, or grab a segment, break it at the contact plane, and retain the portion inside of the device. It also does this with few moving parts in a simple, space-efficient design.

This discovery could be implemented into a coring drill bit to precisely break off and retain any size rock core.

This work was done by Megan Richardson and Justin Lin of Caltech for NASA's Jet Propulsion Laboratory. Further information is contained in a TSP (see page 1). NPO-47444

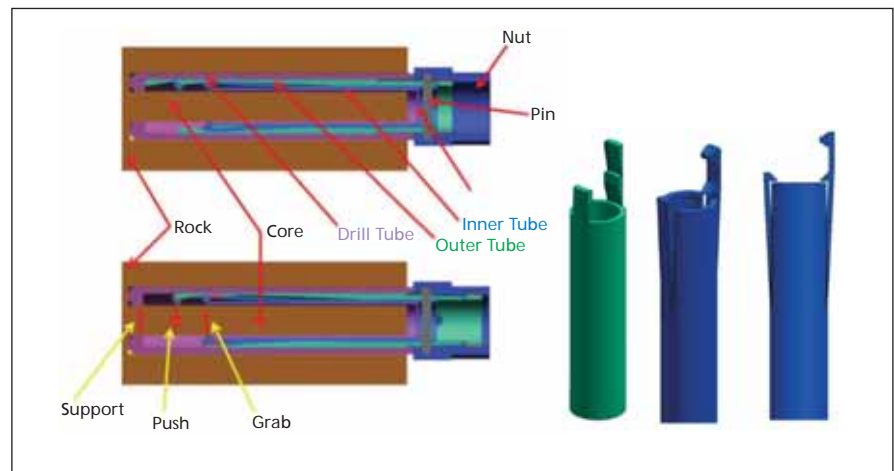
Praying Mantis Bending Core Breakoff and Retention Mechanism

This mechanism has application in sampling cores for analytical tests of geological materials.

NASA's Jet Propulsion Laboratory, Pasadena, California

Sampling cores requires the controlled breakoff of the core at a known location with respect to the drill end. An additional problem is designing a mechanism that can be implemented at a small scale, yet is robust and versatile enough to be used for a variety of core samples.

The new design consists of a set of tubes (a drill tube, an outer tube, and an inner tube) and means of sliding the inner and outer tubes axially relative to each other. Additionally, a sample tube can be housed inside the inner tube for storing the sample. The inner tube fits inside the outer tube, which fits inside the drill tube. The inner and outer tubes can move axially relative to each other. The inner tube presents two lamellae with two opposing grabbing teeth and one pushing tooth. The pushing tooth is offset axially from the grabbing teeth. The teeth can move radially and their motion is controlled by the outer tube. The outer tube presents two lamellae with radial extrusions to control the inner tube lamel-



The Praying Mantis Core Breakoff Mechanism design assembly (left), and (right) the outer (green) and inner tubes (blue).

lae motion. In breaking the core, the mechanism creates two support points (the grabbing teeth and the bit tip) and one push point. The core is broken in bending. The grabbing teeth can also act as a core retention mechanism.

The praying mantis that is disclosed herein is an active core breaking/retention mechanism that requires only one additional actuator other than the drilling actuator. It can break cores that are attached to the borehole bottom as

well as broken cores, and it also acts as a core retention device. The cores are broken at the bottom of the sample tube with a clean cut. The invention uses a core bending principle and does not induce additional axial load on the drill/robotic arm.

This invention is potentially applicable to sample return and *in situ* missions to planets such as Mars and Venus, moons such as Titan and Europa, and comets. It is also applicable to terrestrial applications like forensic sampling and geological sampling in the field.

This work was done by Mircea Badescu, Stewart Sherrit, Yoseph Bar-Cohen, Xiaoqi Bao, and Randel A. Lindemann of Caltech for NASA's Jet Propulsion Laboratory. Further information is contained in a TSP (see page 1). NPO-47356

⚙️ Scoring Dawg Core Breakoff and Retention Mechanism

NASA's Jet Propulsion Laboratory, Pasadena, California

This novel core break-off and retention mechanism consists of a scoring dawg controlled by a set of two tubes (a drill tube and an inner tube). The drill tube and the inner tube have longitudinal concentric holes. The solution can be implemented in an eccentric tube configuration as well where the tubes have eccentric longitudinal holes. The inner tube presents at the bottom two control surfaces for controlling the orientation of the scoring dawg. The drill tube presents a sunk-in profile on the inside of the wall for housing the scoring dawg. The inner tube rotation relative to the drill tube actively controls the orientation of the scoring dawg and hence its penetration and retrieval from the core. The scoring dawg presents a shaft, two axially spaced arms, and a

tooth. The two arms slide on the control surfaces of the inner tube. The tooth, when rotated, can penetrate or be extracted from the core.

During drilling, the two tubes move together maintaining the scoring dawg completely outside the core. After the desired drilling depth has been reached the inner tube is rotated relative to the drill tube such that the tooth of the scoring dawg moves toward the central axis. By rotating the drill tube, the scoring dawg can score the core and so reduce its cross sectional area. The scoring dawg can also act as a stress concentrator for breaking the core in torsion or tension. After breaking the core, the scoring dawg can act as a core retention mechanism.

For scoring, it requires the core to be attached to the rock. If the core is bro-

ken, the dawg can be used as a retention mechanism. The scoring dawg requires a hard-tip insert like tungsten carbide for scoring hard rocks. The relative rotation of the two tubes can be controlled manually or by an additional actuator. In the implemented design solution the bit rotation for scoring was in the same direction as the drilling. The device was tested for limestone cores and basalt cores. The torque required for breaking the 10-mm diameter limestone cores was 5 to 5.8 lb-in. (0.56 to 0.66 N-m).

This work was done by Mircea Badescu, Stewart Sherrit, Yoseph Bar-Cohen, Xiaoqi Bao, and Paul G. Backes of Caltech for NASA's Jet Propulsion Laboratory. Further information is contained in a TSP (see page 1). NPO-47355

⚙️ Rolling-Tooth Core Breakoff and Retention Mechanism

The mechanism has applications in analytical tests of geological materials.

NASA's Jet Propulsion Laboratory, Pasadena, California

Sampling cores requires the controlled breakoff of the core at a known location with respect to the drill end. An additional problem is designing a mechanism that can be implemented at a small scale that is robust and versatile enough to be used for a variety of core samples. This design consists of a set of tubes (a drill tube and an inner tube) and a rolling element (rolling tooth). An additional tube can be used as a sample tube. The drill tube and the inner tube have longitudinal holes with the axes offset from the axis of each tube. The two eccentricities are equal. The inner tube fits inside the drill tube, and the sample tube fits inside the inner tube.

While drilling, the two tubes are positioned relative to each other such that the sample tube is aligned with the drill tube axis and core. The drill tube includes teeth and flutes for cuttings removal. The inner tube includes, at the base, the rolling element implemented as a wheel on a shaft in an eccentric slot. An additional slot in the inner tube and a pin in the drill tube limit



The Rolling-Tooth Design of the core breakoff and retention mechanism (left), and the assembled parts (right).

the relative motion of the two tubes. While drilling, the drill assembly rotates relative to the core and forces the rolling tooth to stay hidden in the slot along the inner tube wall. When the drilling depth has been reached, the drill bit assembly is rotated in the opposite direction, and the rolling tooth is engaged and penetrates into the core. Depending on the strength of the created core, the rolling tooth can score, lock the inner tube rela-

tive to the core, start the eccentric motion of the inner tube, and break the core. The tooth and the relative position of the two tubes can act as a core catcher or core-retention mechanism as well. The design was made to fit the core and hole parameters produced by an existing bit; the parts were fabricated and a series of demonstration tests were performed.

This invention is potentially applicable to sample return and *in situ* missions

to planets such as Mars and Venus, to moons such as Titan and Europa, and to comets. It is also applicable to terrestrial applications like forensic sampling and geological sampling in the field.

This work was done by Mircea Badescu, Donald B. Bickler, Stewart Sherrit, Yoseph Bar-Cohen, Xiaoqi Bao, and Nicolas H. Hudson of Caltech for NASA's Jet Propulsion Laboratory. Further information is contained in a TSP (see page 1). NPO-47354

Vibration Isolation and Stabilization System for Spacecraft Exercise Treadmill Devices

Lyndon B. Johnson Space Center, Houston, Texas

A novel, passive system has been developed for isolating an exercise treadmill device from a spacecraft in a zero-G environment. The Treadmill 2 Vibration Isolation and Stabilization System (T2-VIS) mechanically isolates the exercise treadmill from the spacecraft/space station, thereby eliminating the detrimental effect that high impact loads generated during walking/running would have on the spacecraft

structure and sensitive microgravity science experiments. This design uses a second-stage spring, in series with the first stage, to achieve an order of magnitude higher exercise-frequency isolation than conventional systems have done, while maintaining desirable low-frequency stability performance. This novel isolator design, in conjunction with appropriately configured treadmill platform inertia properties, has

been shown (by on-orbit zero-G testing on-board the International Space Station) to deliver exceedingly high levels of isolation/stability performance.

This work was done by Ian Fialho, Craig Tyer, Bryan Murphy, Paul Cotter, and Sreekumar Thampi of The Boeing Company for Johnson Space Center. For further information contact the JSC Innovation Partnerships Office at (281) 483-3809. MSC-24847-1



Microgravity-Enhanced Stem Cell Selection

This method provides rapid selection and proliferation of stem cells using a hydrofocusing bioreactor.

Goddard Space Flight Center, Greenbelt, Maryland

Stem cells, both embryonic and adult, promise to revolutionize the practice of medicine in the future. In order to realize this potential, a number of hurdles must be overcome. Most importantly, the signaling mechanisms necessary to control the differentiation of stem cells into tissues of interest remain to be elucidated, and much of the present research on stem cells is focused on this goal. Nevertheless, it will also be essential to achieve large-scale expansion and, in many cases, assemble cells in 3D as transplantable tissues. To this end, microgravity analog bioreactors can play a significant role.

Microgravity bioreactors were originally conceived as a tool to study the cellular responses to microgravity. However, the technology can address some of the shortcomings of conventional cell culture systems; namely, the deficiency of mass transport in static culture and high mechanical shear forces in stirred systems. Unexpectedly, the conditions created in the vessel were ideal for 3D cell culture. Recently, investigators have demonstrated the capability of the microgravity bioreactors to expand hematopoietic stem cells compared to

static culture, and facilitate the differentiation of umbilical cord stem cells into 3D liver aggregates.

Stem cells are capable of differentiating into functional cells. However, there are no reliable methods to induce the stem cells to form specific cells or to gain enough cells for transplantation, which limits their application in clinical therapy. The aim of this study is to select the best experimental setup to reach high proliferation levels by culturing these cells in a microgravity-based bioreactor. In typical cell culture, the cells sediment to the bottom surface of their container and propagate as a one-cell-layer sheet. Prevention of such sedimentation affords the freedom for self-assembly and the propagation of 3D tissue arrays.

Suspension of cells is easily achievable using stirred technologies. Unfortunately, in conventional bioreactors, stirring invokes deleterious forces that disrupt cell aggregation and results in cell death. First-generation rotating bioreactors provided rotation on the horizontal axis, which resulted in the suspension of cells without stirring, thus providing a suitable environment to propagate cells without sedimentation to a surface. The rotating-

wall bioreactors did not provide a way to remove air bubbles that were causing shear and disrupting 3D cultures. Johnson Space Center successfully engineered the hydrofocusing bioreactor (HFB) that resolved the problem of removing the air bubbles from the fluid medium of NASA's rotating-wall space bioreactors.

The HFB uses the principle of hydrodynamic focusing that simultaneously produces a low-shear fluid culture environment and a variable hydrofocusing force that can control the movement, location, and removal of suspended cells, tissues, and air bubbles from the bioreactor. The HFB is a rotating, dome-shaped cell culture vessel with a centrally located sampling port and an internal viscous spinner. The vessel and spinner can rotate at different speeds either in the same or opposite directions. Rotation of the vessel and viscous interaction at the spinner generate a hydrofocusing force. Adjusting the differential rotation rate between vessel and spinner controls the magnitude of the force.

This work was done by Pier Paolo Claudio and Jagan Valluri of Goddard Space Flight Center. Further information is contained in a TSP (see page 1). GSC-15807-1

Diagnosis and Treatment of Neurological Disorders by Millimeter-Wave Stimulation

These techniques enable new treatments for neurological disorders and dysfunction.

NASA's Jet Propulsion Laboratory, Pasadena, California

Increasingly, millimeter waves are being employed for telecomm, radar, and imaging applications. To date in the U.S, however, very few investigations on the impact of this radiation on biological systems at the cellular level have been undertaken. In the beginning, to examine the impact of millimeter waves on cellular processes, researchers discovered that cell membrane depolarization may be triggered by low levels of in-

tegrated power at these high frequencies. Such a situation could be used to advantage in the direct stimulation of neuronal cells for applications in neuroprosthetics and diagnosing or treating neurological disorders.

An experimental system was set up to directly monitor cell response on exposure to continuous-wave, fixed-frequency, millimeter-wave radiation at low and modest power levels (0.1 to

100 safe exposure standards) between 50 and 100 GHz. Two immortalized cell lines derived from lung and neuronal tissue were transfected with green fluorescent protein (GFP) that locates on the inside of the cell membrane lipid bi-layer. Oxonol dye was added to the cell medium. When membrane depolarization occurs, the oxonol bound to the outer wall of the lipid bi-layer can penetrate close to the inner wall where

the GFP resides. Under fluorescent excitation (488 nm), the normally green GFP (520 nm) optical signal quenches and gives rise to a red output when the oxonol comes close enough to the GFP to excite a fluorescence resonance energy transfer (FRET) with an output at 620 nm.

The presence of a strong FRET signature upon exposures of 30 seconds to 2 minutes at 5–10 mW/cm² RF power at 50 GHz, followed by a return to the normal 520-nm GFP signal after a few minutes indicating repolarization of the membrane, indicates that low levels of RF energy may be able to trigger non-destructive membrane depolarization without direct cell contact. Such a mechanism could be used to stimulate neuronal cells in the cortex without the need for invasive electrodes as millimeter waves penetrate skin and bone on the order of 1–5

mm in depth. Although 50 GHz could not readily penetrate from the outer skull to the center of the cortex, implants on the outer skull or even on the scalp could reach the outer layer of the cerebral cortex where substantial benefit could be realized from such non-contact type excitation.

The stimulation system described here for cerebral cortex, brainstem, spinal cord, or peripheral nerves includes an implantable housing, a control unit carried by the implantable housing, a millimeter-wave delivery device (including at least one emission site), and at least one millimeter-wave source operatively coupled to the control unit, and coupled to at least one millimeter-wave emission site. Optional components for monitoring of neuronal function can be included, such as an electroencephalographic system, an

electromyographic system, a system for optical or infrared imaging of intrinsic neuronal signals, and/or magnetic resonance imaging/spectroscopy systems.

This work was done by Peter H. Siegel of Caltech and Victor Pikov of HMRI for NASA's Jet Propulsion Laboratory. For more information, contact iaoffice@jpl.nasa.gov.

In accordance with Public Law 96-517, the contractor has elected to retain title to this invention. Inquiries concerning rights for its commercial use should be addressed to:

Innovative Technology Assets Management

JPL

Mail Stop 202-233

4800 Oak Grove Drive

Pasadena, CA 91109-8099

E-mail: iaoffice@jpl.nasa.gov

Refer to NPO-47198, volume and number of this NASA Tech Briefs issue, and the page number.



Passive Vaporizing Heat Sink

Lyndon B. Johnson Space Center, Houston, Texas

A passive vaporizing heat sink has been developed as a relatively lightweight, compact alternative to related prior heat sinks based, variously, on evaporation of sprayed liquids or on sublimation of solids. This heat sink is designed for short-term dissipation of a large amount of heat and was originally intended for use in regulating the temperature of spacecraft equipment during launch or re-entry. It could also be useful in a terrestrial setting in which there is a require-

ment for a lightweight, compact means of short-term cooling. This heat sink includes a hermetic package closed with a pressure-relief valve and containing an expendable and rechargeable coolant liquid (e.g., water) and a conductive carbon-fiber wick. The vapor of the liquid escapes when the temperature exceeds the boiling point corresponding to the vapor pressure determined by the setting of the pressure-relief valve. The great advantage of this heat sink over a melting-paraffin

or similar phase-change heat sink of equal capacity is that by virtue of the $\approx 10\times$ greater latent heat of vaporization, a coolant-liquid volume equal to $\approx 1/10$ of the paraffin volume can suffice.

This work was done by Timothy R. Knowles, Victor A. Ashford, Michael G. Carpenter, and Thomas M. Bier of Energy Science Laboratories, Inc., for Johnson Space Center. For further information, contact the Johnson Commercial Technology Office at (281) 483-3809. MSC-23414-1

Remote Sensing and Quantization of Analog Sensors

This technique has applications in automotive ride and steering sensors, and in industrial vibration and process monitors.

NASA's Jet Propulsion Laboratory, Pasadena, California

This method enables sensing and quantization of analog strain gauges. By manufacturing a piezoelectric sensor stack in parallel (physical) with a piezoelectric actuator stack, the capacitance of the sensor stack varies in exact proportion to the exertion applied by the actuator stack. This, in turn, varies the output frequency of the local sensor oscillator. The output, F_{out} , is fed to a phase detector, which is driven by a stable reference, F_{ref} .

The output of the phase detector is a square waveform, D_{out} , whose duty cycle, t_w , varies in exact proportion according to whether F_{out} is higher or lower than F_{ref} . In this design, should F_{out} be precisely equal to F_{ref} , then the waveform has an exact 50/50 duty cycle.

The waveform, D_{out} , is of generally very low frequency suitable for safe transmission over long distances without corruption. The active portion of the waveform, t_w , gates a remotely located counter, which is driven by a stable oscillator (source) of such frequency as to give sufficient digitization of t_w to the resolution required by the application.

The advantage to this scheme is that it negates the most-common, present method of sending either very low level signals (viz. direct output from the sensors) across great distances (anything over one-half meter) or the need to transmit widely varying higher frequencies over significant distances thereby eliminating interference [both in terms of beat frequency generation and *in-situ* EMI (elec-

tromagnetic interference)] caused by ineffective shielding. It also results in a significant reduction in shielding mass.

This work was done by Karl F. Strauss of Caltech for NASA's Jet Propulsion Laboratory.

In accordance with Public Law 96-517, the contractor has elected to retain title to this invention. Inquiries concerning rights for its commercial use should be addressed to:

*Innovative Technology Assets Management
JPL*

Mail Stop 202-233

4800 Oak Grove Drive

Pasadena, CA 91109-8099

E-mail: iaoffice@jpl.nasa.gov

Refer to NPO-46665, volume and number of this NASA Tech Briefs issue, and the page number.

Phase Retrieval for Radio Telescope and Antenna Control

Goddard Space Flight Center, Greenbelt, Maryland

Phase-retrieval is a general term used in optics to describe the estimation of optical imperfections or "aberrations." The purpose of this innovation is to develop the application of phase retrieval to radio telescope and antenna control

in the millimeter wave band.

Earlier techniques do not approximate the incoherent subtraction process as a coherent propagation. This approximation reduces the noise in the data and allows a straightforward application

of conventional phase retrieval techniques for radio telescope and antenna control.

The application of iterative-transform phase retrieval to radio telescope and antenna control is made by approximating

the incoherent subtraction process as a coherent propagation. Thus, for systems utilizing both positive and negative polarity feeds, this approximation allows both surface and alignment errors to be assessed without the use of additional hardware or laser metrology. Knowledge of

the antenna surface profile allows errors to be corrected at a given surface temperature and observing angle. In addition to imperfections of the antenna surface figure, the misalignment of multiple antennas operating in unison can reduce or degrade the signal-to-noise ratio of the

received or broadcast signals. This technique also has application to the alignment of antenna array configurations.

This work was done by Bruce Dean of Goddard Space Flight Center. Further information is contained in a TSP (see page 1). GSC-15977-1

Helium-Cooled Black Shroud for Subscale Cryogenic Testing

A sheet metal and honeycomb design allows a space-like thermal environment to be maintained around a test item.

Goddard Space Flight Center, Greenbelt, Maryland

This shroud provides a deep-space simulating environment for testing scaled-down models of passively cooling systems for spaceflight optics and instruments. It is used inside a liquid-nitrogen-cooled vacuum chamber, and it is cooled by liquid helium to 5 K. It has an inside geometry of approximately 1.6 m diameter by 0.45 m tall. The inside surfaces of its top and sidewalls have a thermal absorptivity greater than 0.96. The bottom wall has a large central opening that is easily customized to allow a specific test item to extend through it. This enables testing of scale models of realistic passive cooling configurations that feature a very large temperature drop between the deep-space-facing cooled side and the Sun/Earth-facing warm side.

This shroud has an innovative thermal closeout of the bottom wall, so that a test sample can have a hot (room temperature) side outside of the shroud, and a cold side inside the shroud. The combination of this closeout and the very black walls keeps radiated heat from the sample's warm end from entering the shroud, reflecting

off the walls and heating the sample's cold end.

The shroud includes 12 vertical rectangular sheet-copper side panels that are oriented in a circular pattern. Using tabs bent off from their edges, these side panels are bolted to each other and to a steel support ring on which they rest. The removable shroud top is a large copper sheet that rests on, and is bolted to, the support ring when the shroud is closed. The support ring stands on four fiberglass tube legs, which isolate it thermally from the vacuum chamber bottom. The insides of the copper top and side panels are completely covered with 25-mm-thick aluminum honeycomb panels. This honeycomb is painted black before it is epoxied to the copper surfaces. A spiral-shaped copper tube, clamped at many different locations to the outside of the top copper plate, serves as part of the liquid helium cooling loop.

Another copper tube, plumbed in a series to the top plate's tube, is clamped to the sidewall tabs where they are bolted to the support ring. Flowing liquid helium through these tubes cools the entire shroud to 5 K. The entire

shroud is wrapped loosely in a layer of double-aluminized Kapton. The support ring's inner diameter is the largest possible hole through which the test item can extend into the shroud.

Twelve custom-sized trapezoidal copper sheets extend inward from the support ring to within a few millimeters of the test item. Attached to the inner edge of each of these sheets is a custom-shaped strip of Kapton, which is aluminum-coated on the warm-facing (outer) side, and has thin Dacron netting attached to its cold-facing side. This Kapton rests against the test item, but the Dacron keeps it from making significant thermal contact. The result is a non-contact, radiatively reflective thermal closeout with essentially no gap through which radiation can pass. In this way, the part of the test item outside the shroud can be heated to relatively high temperatures without any radiative heat leaking to the inside.

This work was done by James Tuttle, Michael Jackson, Michael DiPirro, and John Francis for Goddard Space Flight Center. Further information is contained in a TSP (see page 1). GSC-15968-1



Receive Mode Analysis and Design of Microstrip Reflectarrays

A new method developed for the design of microstrip reflectarrays is extremely efficient.

NASA's Jet Propulsion Laboratory, Pasadena, California

Traditionally microstrip or printed reflectarrays are designed using the "transmit mode" technique. In this method, the size of each printed element is chosen so as to provide the required value of the reflection phase such that a collimated beam results along a given direction. The reflection phase of each printed element is approximated using an infinite array model. The infinite array model is an excellent engineering approximation for a large microstrip array since the size or orientation of elements exhibits a slow spatial variation.

In this model, the reflection phase from a given printed element is approximated by that of an infinite array of elements of the same size and orientation when illuminated by a local plane wave. Thus the reflection phase is a function of the size (or orientation) of the element, the elevation and azimuth angles of incidence of a local plane wave, and polarization. Typically, one computes the reflection phase of the infinite array as a function of several parameters such as size/orientation, elevation and azimuth angles of incidence, and in some cases for vertical and horizontal polarization. The design requires the selection of the size/orientation of the printed element to realize the required phase by interpolating or curve fitting all the computed data. This is a substantially complicated problem, especially in applications re-

quiring a computationally intensive commercial code to determine the reflection phase. In dual polarization applications requiring rectangular patches, one needs to determine the reflection phase as a function of five parameters (dimensions of the rectangular patch, elevation and azimuth angles of incidence, and polarization). This is an extremely complex problem.

The new method employs the reciprocity principle and reaction concept, two well-known concepts in electromagnetics to derive the receive mode analysis and design techniques. In the "receive mode design" technique, the reflection phase is computed for a plane wave incident on the reflectarray from the direction of the beam peak. In antenna applications with a single collimated beam, this method is extremely simple since all printed elements see the same angles of incidence. Thus the number of parameters is reduced by two when compared to the transmit mode design. The reflection phase computation as a function of five parameters in the rectangular patch array discussed previously is reduced to a computational problem with three parameters in the receive mode. Furthermore, if the beam peak is in the broadside direction, the receive mode design is polarization independent and the reflection phase computation is a func-

tion of two parameters only. For a square patch array, it is a function of the size, one parameter only, thus making it extremely simple.

The present method is substantially less intensive computationally. Since most practical antenna arrays require the design of a broadside beam or a single collimated beam, the receive mode design is expected to be substantially simpler than the traditional transmit mode design. In addition, when a designer needs to generate the reflection phase data using a computer intensive commercial software such as Ansoft HFSS, the reduction of computational effort in the receive mode will result in a substantial saving in design turnaround time. Similarly the receive mode analysis technique has potential to save computer time for large reflectarrays.

Microstrip reflectarrays have desirable features such as ease of design, manufacture, and deployment for application in many space-based radar and remote sensing systems. They are being investigated for many JPL systems such as SWOT (Surface Water Ocean Topography). The receive mode design and analysis technique is expected to find many future applications in NASA.

This work was done by Sembiam Rengarajan of Caltech for NASA's Jet Propulsion Laboratory. For more information, contact iaoffice@jpl.nasa.gov. NPO-47408

Chance-Constrained Guidance With Non-Convex Constraints

This solution can be used for non-convex guidance problems in small-body rendezvous, formation flight, and uninhabited aerial vehicle applications.

NASA's Jet Propulsion Laboratory, Pasadena, California

Missions to small bodies, such as comets or asteroids, require autonomous guidance for descent to these small bodies. Such guidance is made challenging by uncertainty in the position and velocity of the spacecraft, as well as the uncertainty in the gravitational field around the small body. In addition, the require-

ment to avoid collision with the asteroid represents a non-convex constraint that means finding the optimal guidance trajectory, in general, is intractable.

In this innovation, a new approach is proposed for chance-constrained optimal guidance with non-convex constraints. Chance-constrained guidance

takes into account uncertainty so that the probability of collision is below a specified threshold. In this approach, a new bounding method has been developed to obtain a set of decomposed chance constraints that is a sufficient condition of the original chance constraint. The decomposition of the chance constraint

enables its efficient evaluation, as well as the application of the branch and bound method. Branch and bound enables non-convex problems to be solved efficiently to global optimality.

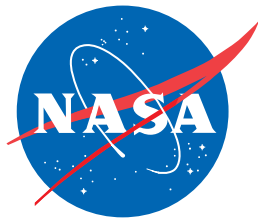
Considering the problem of finite-horizon robust optimal control of dynamic systems under Gaussian-distributed stochastic uncertainty, with state and control constraints, a discrete-time, continuous-state linear dynamics model is assumed. Gaussian-distributed stochastic uncertainty is a more natural model for exogenous disturbances such as wind

gusts and turbulence than the previously studied set-bounded models. However, with stochastic uncertainty, it is often impossible to guarantee that state constraints are satisfied, because there is typically a non-zero probability of having a disturbance that is large enough to push the state out of the feasible region.

An effective framework to address robustness with stochastic uncertainty is optimization with chance constraints. These require that the probability of violating the state constraints (i.e., the probability of failure) is below a user-

specified bound known as the risk bound. An example problem is to drive a car to a destination as fast as possible while limiting the probability of an accident to 10^{-7} . This framework allows users to trade conservatism against performance by choosing the risk bound. The more risk the user accepts, the better performance they can expect.

This work was done by Lars James Blackmore of Caltech and Masahiro Ono and Brian Williams of MIT for NASA's Jet Propulsion Laboratory. For more information, contact iaoffice@jpl.nasa.gov. NPO-47305



National Aeronautics and
Space Administration